DOI: 10.1002/ejoc.200700968

Stereospecific Pseudorotation of Diastereomeric Anti-Apicophilic Spirophosphoranes: A Novel Stereochemical Transformation Involving 10-P-5 Phosphoranes

Satoshi Kojima,*[a] Masaaki Nakamoto,[a] and Kin-ya Akiba*[b]

Keywords: Anti-apicophilicity / Pseudorotation / Phosphoranes / Stereospecificity / Oxidation

A diastereomeric pair of monocyclic apical H-phosphoranes (**2-*exo*** and **2-*exo***) has been prepared from a diastereomeric pair of bicyclic equatorial H-spirophosphoranes (**1**) with *t*BuLi. The thermal cyclization reaction of each diastereomeric apical H-phosphorane gave rise to different diastereomeric *O*-equatorial anti-apicophilic phosphoranes (**3-*exo*** and **3-*endo***, respectively) as single products. On the other hand, the oxidation reaction of each of these apical H-phosphoranes was complementary to the thermal reaction, affording the opposite diastereomeric anti-apicophilic phosphorane (**3-*endo*** and **3-*exo***, respectively) as a single product. The pseudorotation of each of these diastereomeric anti-apicophilic phosphoranes (**3-*exo*** and **3-*endo***) gave rise to different diastereomeric *O*-apical phosphoranes (**4-*exo*** and **4-*endo***, respectively) as single products.

Introduction

Phosphorus plays a vital role in biological systems, such as in DNA-related transformations, and some synthetically useful transformations utilize phosphorus-based reagents. The implications are that many reactions based upon the transformation of the phosphorus moiety involve pentacoordinate (10-P-5) intermediates, and the nature of these 10-P-5 states is strongly related to the reactivity and/or selectivity of the reactions involved.[1] In order to elucidate the general principles relating to 10-P-5 species,[2] many stable model 10-P-5 phosphoranes have been devised and studied. Two important concepts have been deduced from these studies: Apicophilicity,[3,4] a thermodynamic characteristic that rationalizes the relative stability of conceivable diastereomers of which there could, in principle, be up to 20, and pseudorotation (BPR),[5] a kinetic characteristic that rationalizes interconversions between stereoisomeric (or topologically isomeric) phosphoranes. These two features are not unique to phosphorus and are commonly shared by all pentacoordinate compounds that adopt a trigonal-pyramidal structure.

Although there are some rare cases in which an atom of lower electronegativity preferentially occupies an apical position in the presence of an atom of higher electronegativity, all previously known cases involving such species had been created by imposing special thermodynamic modifications.[6] However, by utilizing the Martin ligand[7] we have recently succeeded in preparing spirophosphoranes in which the more apicophilic oxygen atom and the less apicophilic carbon atom have reversed places to give "anti-apicophilic" phosphoranes (*O*-equatorial *C*-apical phosphoranes) such as **I** and **II** (Figure 1), although they are not particularly stable thermodynamically. Actually, these unique species are much higher in energy (estimated to be more than 14 kcal mol^{-1} less stable) than their *O*-apical *C*-equatorial stereoisomers (phosphoranes with a configuration in which the bidentate binding of the ligand is reversed) and thus cannot exist under equilibrating conditions.[8] Owing to this low stability relative to its *O*-apical isomer, unorthodox methods for their preparation were required.[8a,8b] In connection with this previous work, we have examined diastereomeric anti-apicophilic phosphoranes analogous to **I** by using a modified Martin ligand in which a methyl group replaces one of the trifluoromethyl groups in one of the bidentate Martin ligands. In doing so we found that pseudorotation of the *O*-equatorial isomers to

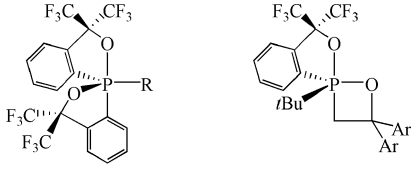

Figure 1. Examples of anti-apicophilic phosphoranes.

[a] Department of Chemistry, Graduate School of Science, Hiroshima University
1-3-1 Kagamiyama, Higashi-Hiroshima 739-8526, Japan
Fax: +81-82-424-0727
E-mail: skojima@sci.hiroshima-u.ac.jp
[b] Advanced Research Center for Science and Engineering, Waseda University
3-4-1 Ohkubo, Shinjuku-ku, Tokyo 169-8555, Japan

O-apical isomers could be carried out in a stereospecific manner. Furthermore, we have discovered that these anti-apicophilic phosphoranes could also be formed in a stereospecific manner by two methods, thermal and oxidative cyclization, which incidentally were completely complementary to each other. The details are described herein.

Results and Discussion

According to the method previously described,[7,8b–8d] monocyclic P–H (apical) phosphoranes **2-*exo***[9] [J_{PH} ($CDCl_3$) = 291 Hz] and **2-*exo*** [J_{PH} ($CDCl_3$) = 273 Hz], which are diastereomeric by virtue of an asymmetric carbon atom (denoted with an *) in the monodentate aryl substituent, were prepared (*endo*/*exo* = 24:76) by the reaction of H-phosphorane **1** with about 3 equiv. of *t*BuLi (Scheme 1). As one might expect from the highly electronegative nature of the Martin ligand compared with that of the modified asymmetric ligand, only diastereomeric phosphoranes bearing the Martin ligand as the bidentate ligand could be observed. Pseudorotation between the two isomeric phosphoranes **2-*exo*** and **2-*exo*** was found to be surprisingly slow at room temperature, although they were monocyclic, thus allowing separation by TLC.[10] The relative stereochemistry of the diastereomers was established by X-ray analysis of the **2-*exo*** diastereomer recrystallized from MeCN (Figure 2). This species was shown to have an (R_P*R_C*) configuration with intermolecular hydrogen-bonding between the hydroxy group and a molecule of MeCN. Dissolution of each of these diastereomers in $CDCl_3$ led to mixtures of intramolecular (intra) and intermolecular (inter) hydrogen-bonded isomers with intra/inter ratios of 74 (δ_P = –14.8 ppm):26 (δ_P = –45.7 ppm) and 22 (δ_P = –17.8 ppm):78 (δ_P = –40.6 ppm) for **2-*exo*/2-*exo***.[11]

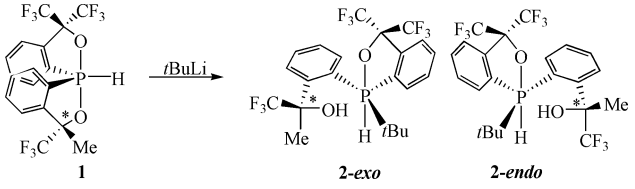

Scheme 1. Preparation of **2-*exo*** and **2-*exo***.

For the cyclization reaction, first of all, the original method, namely the thermal reaction in which pyridine was found to promote the formation of anti-apicophilic phosphoranes, was examined. In spite of the fact that there was a difference in the electronic character of the diastereomeric apical H-phosphoranes compared with their counterparts bearing two Martin ligands, the thermal cyclization reaction proceeded similarly and gave only anti-apicophilic phosphoranes as the products upon heating at 60 °C in pyridine. Furthermore, it was found that the thermal cyclization reaction of the major diastereomer **2-*exo*** resulted in the exclusive formation of **3-*exo*** (δ_P = 3.0 ppm), whereas the other diastereomer, **2-*exo***, gave solely the opposite diastereomer, **3-*endo*** (δ_P = 1.6 ppm), under similar reaction conditions (Scheme 2).

As for the modified method of preparation using an oxidizing agent, only the anti-apicophilic phosphorane was observed, just as in the thermal reaction, by treating **2** with *n*BuLi followed by iodine. Interestingly, however, the oxidative cyclization of **2** gave the diastereomeric spirophosphorane **3** opposite to that obtained in the thermal reaction as the exclusive product. That is, **2-*exo*** gave **3-*endo***, and **2-*exo*** afforded **3-*exo***. Thus, not only were both cyclization protocols stereospecific, but they were also completely complementary to each other.

The stereochemistry of **3-*exo*** could be assigned by the presence of a characteristic through-space F–F coupling (J = 6.6 Hz) in the ^{19}F NMR spectrum between the two CF_3 groups on separate ligands that face each other[12] and was confirmed by X-ray structure analysis (Figure 2). This coupling was not observed for **3-*endo*** which has a methyl group facing a CF_3 group instead. Although it is possible for **3-*exo*** and **3-*endo*** to exist in equilibrium with their one-step pseudorotamers **3′-*exo*** (with *t*Bu as the pivot, Scheme 3) and **3′-*endo*** (not shown), respectively, no such isomer nor a dynamic process corresponding to a one-step pseudorotation could be observed for either diastereomer even at –80 °C by VT-NMR spectroscopy in toluene. This indicates that **3-*exo*** and **3-*endo*** are at least 2.7 kcal mol^{-1}[13]

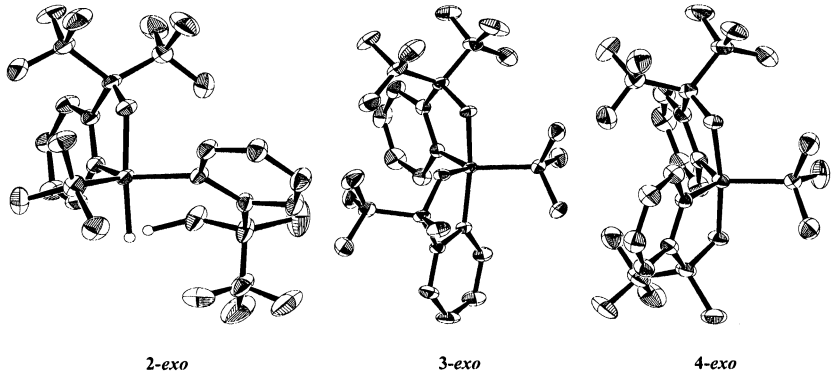

Figure 2. ORTEP drawings of **2-*exo***, **3-*exo***, and **4-*exo*** showing the thermal ellipsoids at the 30% probability level. All hydrogen atoms other than P1–H1 and O2–H2 for **2-*exo*** have been omitted for clarity. The solvent molecule MeCN incorporated into **2-*exo*** has also been omitted for clarity.

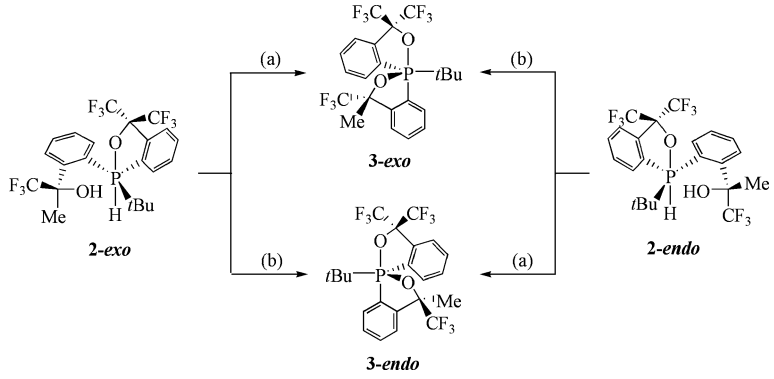

Scheme 2. Stereospecific and complementary formation of **3-*exo*** and **3-*endo***. (a) pyridine, 60 °C; (b) *n*BuLi (2 equiv.), then I_2.

more stable than **3′-*exo*** and **3′-*endo***, respectively. This is clearly a consequence of the high apicophilicity of the oxygen atom in the Martin ligand. Unlike in the case of symmetrical phosphoranes bearing two Martin ligands, the two $^1J_{PC(aryl)}$ values could be observed separately (**3-*endo***: $^1J_{PC(aryl)}$ = 107 and 16 Hz; **3-*exo***: $^1J_{PC(aryl)}$ = 123 and 16 Hz) with the smaller values corresponding to the coupling constants for the apical carbon atoms. Thus, it turns out that our earlier assumption of a coupling constant of about 16 Hz for the coupling between the phosphorus atom and the apical aryl carbon atom was correct.[8e]

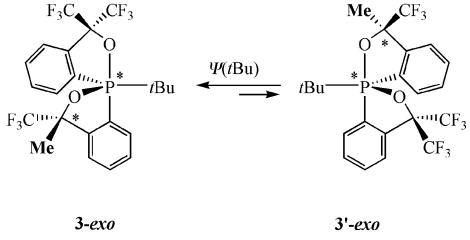

Scheme 3. Equilibrium between **3-*exo*** and **3′-*exo***.

The stereochemical results for the thermal reaction are in very good agreement with our previous assumption that ring closure of the P–H (apical) compounds occurs while maintaining the ground-state configuration with the oxygen atom of the ring-opened unsymmetrical aryl group attacking the phosphorus atom from the side opposite the most electron-withdrawing substituent in the equatorial plane (aryl in this case), as depicted for **2-*exo*** in Scheme 4.[8e] Thus, the initially formed anti-apicophilic phosphorane would be the unobserved **3′-*exo***, which undergoes pseudorotation to the observed isomer **3-*exo***.

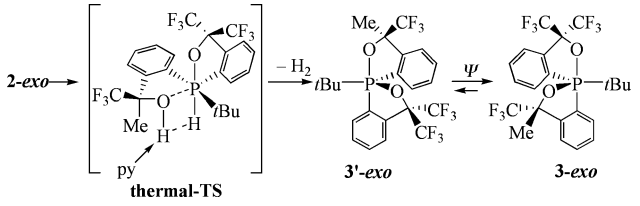

Scheme 4. Plausible mechanism for the formation of **3-*exo*** under thermal conditions.

For the oxidative cyclization process, the following mechanism, exemplified by the reaction of **2-*exo***, would seem rational (Scheme 5). The dianionic species **A** generated by deprotonation of **2-*exo*** undergoes dissociation of the P–O (Martin ligand) bond to give tricoordinate **B** which equilibrates to a mixture that includes phosphane **B′**, phosphinides **C** and **D**, and possibly 12-P-5 species **E**, all four of which maintain the same configuration involving three

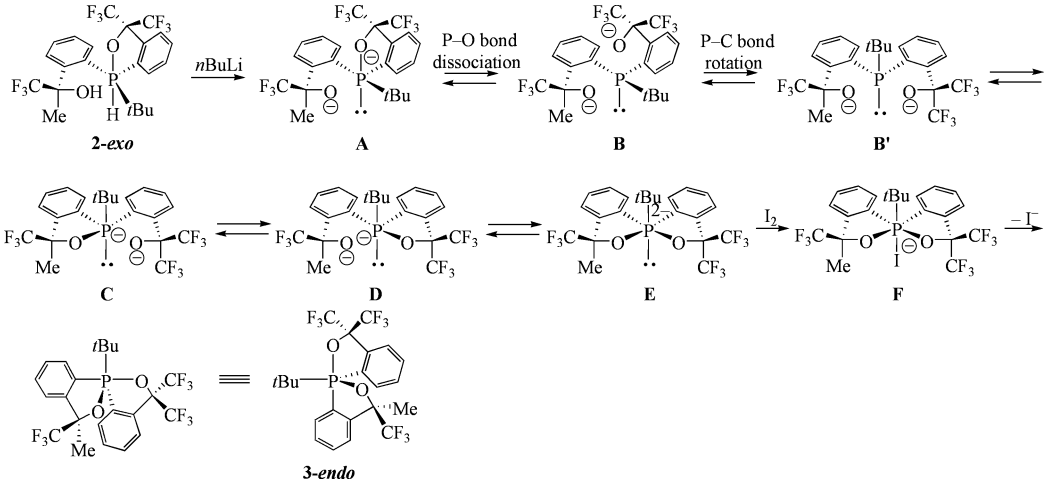

Scheme 5. Plausible mechanism for the formation of **3-*endo*** under oxidative conditions.

P–C bonds and a lone pair on P [in the depicted case: (*S*) stereochemistry], just like an ordinary trivalent P species. In these conformations, the negatively charged oxygen atoms could be stabilized by interaction with the $\sigma^*_{P-C(aryl)}$ orbitals. Whichever may be the reactive species, all could lead to the same intermediate **F** upon oxidation by I_2, which subsequently could give **3-*endo*** upon loss of I^-.

The thermal pseudorotation of *O*-equatorial spirophosphoranes **3-*exo*** and **3-*endo*** in *p*-xylene proceeded stereospecifically to give *O*-apical isomers **4-*exo*** (δ_P = –13.3 ppm) and **4-*endo*** (δ_P = –16.5 ppm), respectively (Scheme 6). The relative stereochemistries of the two diastereomers of **4** were determined by difference NOE and confirmed by X-ray structure analysis of **4-*exo*** (Figure 2).

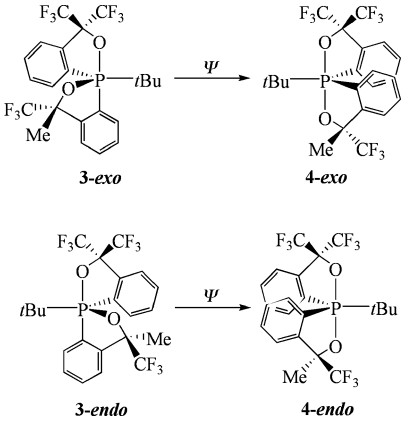

Scheme 6.

In order to determine whether there was a preference between the two stereospecific pseudorotation processes (**3-*exo*** to **4-*exo*** and **3-*endo*** to **4-*endo***), a kinetic examination was carried out by monitoring the change in the ratio of **3/4** as a function of time by ^{19}F NMR spectroscopy. Kinetic measurements of the processes in *p*-xylene gave rise to the activation parameters of $\Delta G^{\ddagger}_{298}$ = 29.1 ± 0.1 kcal mol^{-1}, $\Delta H^{\ddagger}$ = 28.3 ± 0.1 kcal mol^{-1}, and $\Delta S^{\ddagger}$ = –3.3 ± 0.2 cal^{-1} mol^{-1} K^{-1} for the *exo* series and $\Delta G^{\ddagger}_{298}$ = 27.4 ± 0.2 kcal mol^{-1}, $\Delta H^{\ddagger}$ = 26.1 ± 0.1 kcal mol^{-1}, and $\Delta S^{\ddagger}$ = –4.6 ± 0.4 cal^{-1} mol^{-1} K^{-1} for the *endo* series, which indicates that the pseudorotation of **3-*endo*** is faster. Changing the solvent did not lead to a dramatic change in the pseudorotation rate.[14] Based on the facts that there was essentially no solvent effect and that the activation entropy was small, it is likely that bond dissociation is not involved in the rate-determining step and rationalization using the widely recognized Berry pseudorotation mechanism should be appropriate (Tables 1 and 2).[15]

The unique stereomutation observed here can be completely accounted for by using the Desargus–Levi diagram which describes the complete pseudorotation scheme.[16,17] The spirocyclic nature of the phosphoranes reduces the number of possible pathways to those depicted with solid lines.[18] The pathways that the *O*-equatorial isomers follow can be reasonably explained by assuming trigonal-bipyramidal structures as energy maxima for the high-energy pseudorotation steps that involve the formation of strained isomers with a bidentate ligand in the equatorial plane (Figure 3).[2a,19]

Table 1. The rates of pseudorotation for **3-*exo*** and **3-*endo***.[a,b]

Solvent	*T* [K]	Rate [s^{-1}]	
		3-*exo* to **4-*exo***	**3-*exo*** to **4-*exo***
DMSO	363	(1.04 ± 0.01) × 10^{-5}	(9.31 ± 0.03) × 10^{-5}
PhCN	363	(1.21 ± 0.01) × 10^{-5}	(9.84 ± 0.16) × 10^{-5}
p-Xylene	333	–	(5.40 ± 0.06) × 10^{-6}
	343	(1.35 ± 0.03) × 10^{-6}	(1.79 ± 0.01) × 10^{-5}
	353	–	(5.50 ± 0.01) × 10^{-5}
	363	(1.39 ± 0.01) × 10^{-5}	(1.55 ± 0.01) × 10^{-4}
	373	(4.17 ± 0.01) × 10^{-5}	(4.11 ± 0.04) × 10^{-4}
	383	(1.13 ± 0.01) × 10^{-4}	–
	393	(3.04 ± 0.02) × 10^{-4}	–

[a] The process was monitored by ^{19}F NMR spectroscopy. [b] Errors are given as standard deviations.

Table 2. Activation parameters for the pseudorotation of **3-*exo*** and **3-*endo***.[a,b]

	$\Delta H^{\ddagger}$ [kcal mol^{-1}]	$\Delta S^{\ddagger}$ [cal^{-1} mol^{-1} K^{-1}]	$\Delta G^{\ddagger}_{298}$ [kcal mol^{-1}]
3-*exo* to **4-*exo***	28.3 ± 0.01	–3.3 ± 0.2	29.2 ± 0.10
3-*endo* to **4-*endo***	26.1 ± 0.01	–4.6 ± 0.4	27.4 ± 0.20

[a] *p*-Xylene was used as the solvent. [b] Errors are given as standard deviations.

Considerations of ring strain and apicophilicity would put isomer stability in the order of ***45*(*54*)** < ***53*(*35*)** < ***25*(*52*)** < ***15*(*51*)** < ***34*(*43*)** < ***23*(*32*)** < ***41*(*14*)** < ***21*(*12*)** (Figure 3). Thus, the diagram can be used to predict that pseudorotation of **3-*exo*** (***14***) leads to **4-*exo*** (***12***) through the path involving ***14–32–51–43–12***, whereas that of **3-*endo*** (***41***) gives rise to **4-*endo*** (***21***) via ***41–23–15–34–21***, which agrees well with the experimentally observed results. Complete stereospecificity can thus be attributed to the difference in stability between ***25*(*52*)** and ***15*(*51*)**. The latter state should be more stable owing to the presence of a more electronegative oxygen atom in an apical site. This difference in stability, according to oxygen atoms of differing electronegativity, parallels that between **3** and **3′** already discussed (>2.7 kcal mol^{-1}, see above). Thus, from the thermodynamic relationship between one-step pseudorotamers of **3**, it is not necessarily peculiar that the two pseudorotation processes were completely stereospecific. On the other hand, if the difference in electronegativity between the two oxygen atoms were to be reduced, there would be a possibility that the pseudorotation processes would no longer be stereospecific.

Conclusions

We have succeeded for the first time in preparing a diastereomeric pair of anti-apicophilic phosphoranes. The preparation could be carried out in a stereospecific manner by using either thermal or oxidative conditions, and incidentally the two methods turned out to be stereochemically completely complementary to each other. Furthermore,

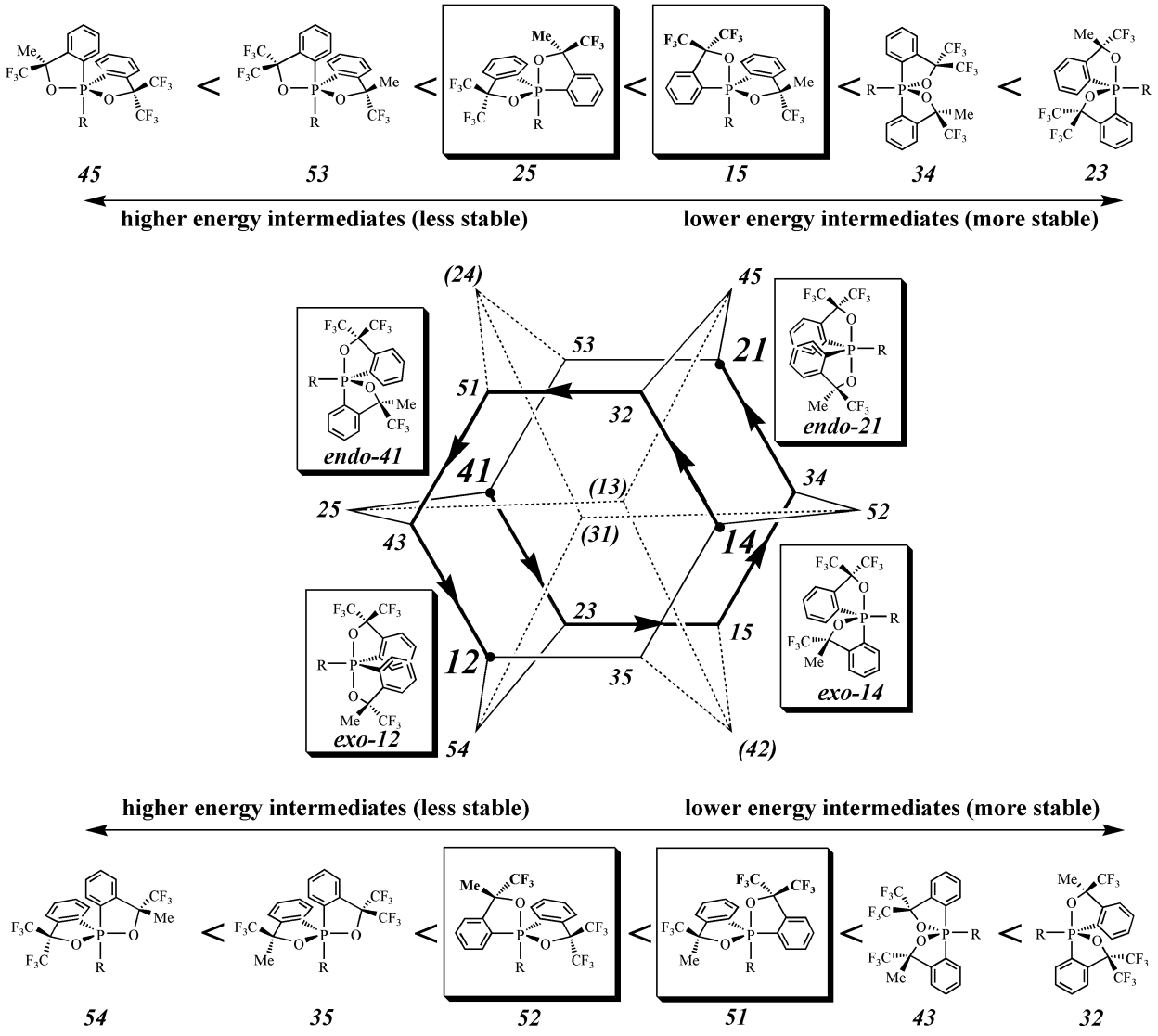

Figure 3. Desargus–Levi diagram for spirophosphoranes. Trigonal-bipyramidal species are shown as vertices. Pathways involving ***13***, ***31***, ***24***, and ***42*** are shown as dotted lines.

pseudorotation of the diastereomeric anti-apicophilic phosphoranes also turned out to be stereospecific. These novel results should shed some light on the not well understood multistep pseudorotation process of not only 10-P-5 phosphoranes but also pentacoordinate species in general.

Experimental Section

General: Melting points were measured with a Yanaco micro-melting point apparatus and are uncorrected. ^{1}H (400 MHz), ^{13}C (100 MHz), ^{19}F (376 MHz), and ^{31}P NMR (162 MHz) spectra were recorded with a JEOL EX-400 spectrometer. ^{1}H NMR chemical shifts (δ) are given in ppm downfield from Me_4Si, determined by residual chloroform (δ = 7.26 ppm). ^{13}C NMR chemical shifts (δ) are given in ppm downfield from Me_4Si, determined by [D]chloroform (δ = 77.0 ppm). ^{19}F NMR chemical shifts (δ) are given in ppm downfield from external $CFCl_3$. ^{31}P NMR chemical shifts (δ) are given in ppm downfield from external 85% H_3PO_4. Elemental analyses were performed with a Perkin-Elmer 2400 CHN elemental analyzer. All reactions were carried out under N_2 or Ar. THF and Et_2O were freshly distilled from Na/benzophenone, *n*-hexane was distilled from Na, and all other solvents were distilled from CaH_2. Preparative thin-layer chromatography was carried out on plates of Merck silica gel 60 GF254. Merck silica gel 60 was used for column chromatography.

[*TBPY*-5-15]-1-*tert*-Butyl-1-hydro-1-[2-(2,2,2-trifluoro-1-hydroxy-1-methylethyl)phenyl]-3,3-bis(trifluoromethyl)-3*H*-2,1λ^5-benzoxaphosphole (2-*exo* and 2-*endo*): *t*BuLi in pentane (1.9 mL, 1.12 M solution) was added to a solution of diastereomeric P–H spirophosphorane **1** (330 mg, 0.71 mmol, ***exo*/*endo*** = 2:98) in toluene (8 mL) at 0 °C. After stirring for 1 h, the solution was quenched with aqueous 1 M HCl and extracted with diethyl ether (3 × 10 mL). The combined organic layers were dried with $MgSO_4$ and filtered. The organic solvent was evaporated in vacuo to give a crude mixture of **2-*exo*/2-*exo*** (diastereomeric ratio 26:74). Purification and diastereomeric resolution were accomplished by thin-layer chromatography (silica gel; hexane/CH_2Cl_2, 3:1) followed by recrystallization from acetonitrile to give **2-*exo*** (32 mg, 8%) and **2-*exo*** (180 mg, 45%) with incorporation of a solvent molecule.

2-*exo*: M.p. 91 °C. ^{1}H NMR ($CDCl_3$): rotational isomer **a**: δ = 1.18 (d, J = 19.5 Hz, 9 H), 1.60 (s, 3 H), 5.94 (d, $^2J_{PH}$ = 291 Hz, 1 H), 7.20–7.45 (m, 5 H), 7.50–7.80 (m, 2 H), 8.57 (m, 1 H) ppm; rotational isomer **b**: δ = 1.38 (d, J = 23.0 Hz, 9 H), 1.60 (s, 3 H), 5.81 (d, $^2J_{PH}$ = 291 Hz, 1 H), 7.20–7.45 (m, 5 H), 7.50–7.80 (m, 2 H), 8.57 (m, 1 H) ppm. ^{19}F NMR ($CDCl_3$): rotational isomer **a**: δ = –79.6 (s, 3 F), –75.9 (q, J = 9.8 Hz, 3 F), –74.1 (q, J = 9.8 Hz, 3 F) ppm; rotational isomer **b**: δ = –78.2 (q, J = 6.8 Hz, 3 F), –76.1 (qq, J = 6.8, 9.8 Hz, 3 F), –73.5 (q, J = 9.8 Hz, 3 F) ppm. ^{31}P NMR ($CDCl_3$): rotational isomer **a**: δ = –40.6 ppm; rotational isomer **b**: δ = –17.8 ppm. $C_{24}H_{25}F_9NO_2P$ (561.06): calcd. C 51.37, H 4.49, N 2.50; found C 51.56, H 4.42, N 2.26.

2-*endo*: ^{1}H NMR ($CDCl_3$): rotational isomer **a**: δ = 1.15 (d, J = 20.0 Hz, 9 H), 1.86 (s, 3 H), 5.99 (d, $^2J_{PH}$ = 272 Hz, 1 H), 7.12–7.82 (m, 5 H), 7.95–8.02 (m, 2 H), 8.65 (m, 1 H) ppm rotational isomer **b**: δ = 1.39 (d, J = 23.4 Hz, 9 H), 1.86 (s, 3 H), 5.86 (d, $^2J_{PH}$ = 268 Hz, 1 H), 7.12–7.82 (m, 5 H), 7.95–8.02 (m, 2 H), 8.65 (m, 1 H) ppm. ^{19}F NMR ($CDCl_3$): rotational isomer **a**: δ = –78.1 (s, 3 F), –75.7 (q, J = 9.3 Hz, 3 F), –74.1 (q, J = 9.3 Hz, 3 F) ppm; rotational isomer **b**: δ = –79.5 (s, 3 F), –75.5 (q, J = 9.9 Hz, 3 F), –73.7 (q, J = 9.9 Hz, 3 F) ppm. ^{31}P NMR ($CDCl_3$): rotational isomer **a**: δ = –45.7 ppm; rotational isomer **b**: δ = –14.9 ppm.

[*TBPY*-5-12]-1-*tert*-Butyl-3′-methyl-3,3,3′-tris(trifluoromethyl)-1,1′-spirobi[3*H*-2,1λ^5-benzoxaphosphole] (3-*exo* and 3-*endo*): A solution of **2-*exo*** (102 mg, 0.20 mmol) in pyridine (0.6 mL) was heated at 60 °C for 5 h. The solution was quenched with 1 M aq. HCl and extracted with diethyl ether (3 × 10 mL). The combined organic layers were dried with $MgSO_4$ and then concentrated in vacuo. Purification by PTLC (SiO_2; hexane/CH_2Cl_2, 2:1) quantitatively gave **3-*exo***. Crystals (90 mg, 88%) suitable for X-ray analysis were obtained by recrystallization from hexane/diethyl ether. The same procedure was used for the preparation of the other diastereomer, **3-*endo***.

3-*exo*: M.p. 118–128 °C. ^{1}H NMR ($CDCl_3$): δ = 1.18 (d, J = 10.5 Hz, 9 H), 1.80 (s, 3 H), 7.44–7.51 (m, 4 H), 7.62 (m, 1 H), 7.80 (m, 1 H), 7.86 (m, 1 H), 7.99 (dd, J = 10.3, 8.3 Hz, 1 H) ppm. ^{19}F NMR ($CDCl_3$): δ = –81.3 (q, J = 6.6 Hz, 3 F), –75.6 (qq, J = 6.6, 9.9 Hz, 3 F), –73.3 (q, J = 9.9 Hz, 3 F) ppm. ^{31}P NMR ($CDCl_3$): δ = 3.0 ppm. ^{13}C NMR ($CDCl_3$): δ = 21.9 (d, J = 5.5 Hz, CF_3CCH_3), 29.4 (*t*Bu), 43.7 (d, J = 116 Hz), 124.2 (d, J = 5.5 Hz, arom. *C*H), 125.4 (d, J = 12.9 Hz, arom. *C*H), 126.9 (d, J = 5.5 Hz, arom. *C*H), 129.7, 130.2 (d, J = 14.7 Hz, arom. *C*H), 131.5 (d, J = 7.3 Hz, arom. *C*H), 132.8, 136.0 (d, J = 14.8 Hz, arom. *C*H), 132.5 (d, J = 123.1 Hz, arom.), 137.3 (d, J = 16.5 Hz, arom.), 139.5 (d, J = 13.1 Hz, arom.), 140.1 (d, J = 33.1 Hz, arom.), 122.6 (q, J = 287 Hz, *C*F_3), 123.3 (dq, J = 11, 288 Hz, *C*F_3), 124.4 (q, J = 285 Hz, *C*F_3) ppm; the benzyl carbon atoms could not be assigned. $C_{22}H_{20}F_9O_2P$ (518.37): calcd. C 50.98, H 3.89; found C 50.96, H 3.62.

3-*endo*: M.p. 142–148 °C. ^{1}H NMR ($CDCl_3$): δ = 1.24 (d, J = 20.5 Hz, 9 H), 1.44 (s, 3 H), 7.47 (m, 4 H), 7.58 (t, J = 6.3 Hz, 1 H), 7.74 (d, J = 7.3 Hz, 1 H), 7.81 (m, 1 H), 7.89 (t, J = 8.3 Hz, 1 H) ppm. ^{19}F NMR ($CDCl_3$): δ = –79.3 (s, 3 F), –74.7 (q, J = 9.9 Hz, 3 F), –73.7 (q, J = 9.9 Hz, 3 F) ppm. ^{31}P NMR ($CDCl_3$): δ = 1.6 ppm. ^{13}C NMR ($CDCl_3$): δ = 23.1 (CF_3CCH_3), 29.8 (*t*Bu), 43.7 (d, J = 114 Hz), 123.7 (d, J = 7.4 Hz, arom. *C*H), 125.3 (d, J = 11.0 Hz, arom. *C*H), 126.8 (d, J = 7.4 Hz, arom. *C*H), 129.8 (d, J = 11.1 Hz, arom. *C*H), 130.1, 132.2, 132.4 (d, J = 9.2 Hz, arom. *C*H), 135.0 (d, J = 14.7 Hz, arom. *C*H), 134.8 (d, J = 106.6 Hz, arom.), 136.2 (d, J = 16.5 Hz, arom.), 138.2 (d, J = 34.2 Hz, arom.), 141.0 (d, J = 14.7 Hz, arom.), 122.8 (q, J = 288 Hz, *C*F_3), 123.0 (q, J = 285 Hz, *C*F_3), 125.0 (dq, J = 9.2, 285 Hz, *C*F_3) ppm; the benzyl carbon atoms could not be assigned. $C_{22}H_{20}F_9O_2P$ (518.37): calcd. C 50.98, H 3.89; found C 51.02, H 3.64.

[*TBPY*-5-11]-1-*tert*-Butyl-3′-methyl-3,3,3′-tris(trifluoromethyl)-1,1′-spirobi[3*H*-2,1λ^5-benzoxaphosphole] (4-*exo* and 4-*endo*): A solution of **3-*exo*** (102 mg, 0.20 mmol) in *p*-xylene (0.6 mL) was heated at 90–120 °C for 5–30 h. The solvent was evaporated in vacuo. Purification by PTLC (silica gel; hexane) quantitatively gave **4-*exo***. Crystals suitable for X-ray analysis were obtained by recrystallization from hexane/diethyl ether. The same procedure was used for the preparation of the other diastereomer, **4-*endo***.

4-*exo*: M.p. 161–162 °C. ^{1}H NMR ($CDCl_3$): δ = 1.10 (d, J = 19.1 Hz, 9 H), 1.78 (s, 3 H), 7.44–7.67 (m, 6 H), 8.33–8.45 (m, 2 H) ppm. ^{19}F NMR ($CDCl_3$): δ = –79.7 (s, 3 F), –74.9 (q, J = 9.9 Hz, 3 F), –73.3 (q, J = 9.9 Hz, 3 F) ppm. ^{31}P NMR ($CDCl_3$): δ = –13.3 ppm. ^{13}C NMR ($CDCl_3$): δ = 20.7 (CF_3CCH_3), 28.4 (*t*Bu), 39.7 (d, J = 110 Hz, *t*Bu), 123.2 (d, J = 15 Hz), 124.0 (d, J = 15 Hz), 129.3 (d, J = 13 Hz), 130.5 (d, J = 13 Hz), 132.4 (d, J = 20 Hz), 132.5 (d, J = 24 Hz), 136.6 (d, J = 9 Hz), 137.6 (d, J = 9 Hz), 131.2 (d, J = 156 Hz), 133.7 (d, J = 165 Hz), 136.2 (d, J = 18 Hz), 145.0 (d, J = 22 Hz), 122.7 (q, J = 288 Hz, *C*F_3), 122.9 (q, J = 287 Hz, *C*F_3), 125.2 (q, J = 287 Hz, *C*F_3) ppm; the benzyl carbon atoms could not be assigned. $C_{22}H_{20}F_9O_2P$ (518.37): calcd. C 50.98, H 3.89; found C 51.19, H 3.95.

4-*endo*: M.p. 144–145 °C. ^{1}H NMR ($CDCl_3$): δ = 1.16 (d, J = 19.5 Hz, 9 H), 1.45 (s, 3 H), 7.44–7.54 (m, 4 H), 7.63 (m, 2 H), 8.32 (t, J = 8.8 Hz, 1 H), 8.44 (d, J = 5.8 Hz, 1 H) ppm. ^{19}F NMR ($CDCl_3$): δ = –77.5 (s, 3 F), –74.3 (q, J = 9.9 Hz, 3 F), –72.7 (q, J = 9.9 Hz, 3 F) ppm. ^{31}P NMR ($CDCl_3$): δ = –16.5 ppm. ^{13}C NMR ($CDCl_3$): δ = 24.9 (CF_3CCH_3), 28.4 (*t*Bu), 40.7 (d, J = 118 Hz, *t*Bu), 121.9 (d, J = 16 Hz), 124.3 (d, J = 15 Hz), 129.1 (d, J = 13 Hz), 130.5 (d, J = 15 Hz), 132.5 (d, J = 28 Hz), 132.6 (d, J = 28 Hz), 136.9 (d, J = 7 Hz), 137.5 (d, J = 9 Hz), 130.3 (d, J = 156 Hz), 134.3 (d, J = 158 Hz), 137.0 (d, J = 15 Hz), 146.2 (d, J = 20 Hz,), 122.7 (q, J = 283 Hz, *C*F_3), 122.9 (q, J = 281 Hz, *C*F_3), 125.5 (q, J = 281 Hz, *C*F_3) ppm; the benzyl carbon atoms could not be assigned. $C_{22}H_{20}F_9O_2P$ (518.37): calcd. C 50.98, H 3.89; found C 51.10, H 3.89.

Kinetic Measurements: Samples (ca. 15 mg) dissolved in freshly distilled solvent (0.5–0.6 mL) were separately sealed in NMR tubes under N_2. The reactions were monitored by measuring ^{19}F NMR integrals in a variable-temperature mode, and the specified temperatures were maintained throughout each set of measurements (error within ±1 °C).

X-ray Crystal Structure Determination of 2-*exo*, 3-*exo*, and 4-*exo*: Crystals suitable for X-ray structure determination were mounted on a Mac Science MXC3 diffractometer and irradiated with graphite-monochromated Cu-K_α radiation (λ = 1.54178 Å) for data collection for **2-*exo*** and **3-*exo***, and graphite-monochromated Mo-K_α radiation (λ = 0.71073 Å) for data collection for **4-*exo***. Lattice parameters were determined by least-squares fitting of 31 reflections for all compounds in the range $51° < 2\theta < 60°$. Data were collected using the $2\theta/\omega$ scan mode. All data were corrected for absorption[20] and extinction.[21] The structures were solved by a direct method and refined by full-matrix least-squares methods with the TeXsan program.[22] All non-hydrogen atoms were refined with anisotropic thermal parameters. All hydrogen atoms other than that directly bonded to the phosphorus atom in **2-*exo*** were included in the refinement at calculated positions (C–H 1.0 Å) riding on their carrier atoms with isotropic thermal parameters. The hydrogen bonded directly to the phosphorus atom in **2-*exo*** was located by using a difference Fourier map. CCDC-628118 (**2-*exo***), -628119 (**3-*exo***), and -628120 (**4-*exo***) contain the supplementary crystallographic

data for this paper. These data can be obtained free of charge from The Cambridge Crystallographic Data Centre via www.ccdc.cam.ac.uk/data_request/cif.

Acknowledgments

The authors are indebted to Dr. Shiro Matsukawa for assistance in the X-ray structural analysis. The authors are grateful to Central Glass Co. Ltd. for a generous gift of hexafluorocumyl alcohol. Partial support of this work provided by the Ministry of Education, Culture, Sports, Science, and Technology of the Japanese Government through a Grant-in-Aid for Scientific Research (Nos. 09239103, 09440218, 11166248, 11304044, and 12304044) is acknowledged.

[1] a) F. H. Westheimer, *Acc. Chem. Res.* **1968**, *1*, 70–78; b) G. R. J. Thatcher, R. Kluger, *Adv. Phys. Org. Chem.* **1989**, *25*, 99–265, and references cited therein.

[2] a) R. R. Holmes, *Pentacoordinated Phosphorus – Structure and Spectroscopy*, ACS Monographs 175, 176, American Chemical Society, Washington, DC, **1980**, vols. I, II; b) N. A. Polezhaeva, R. A. Cherkasoz, *Usp. Khim.* **1985**, *54*, 1899–1939; c) L. N. Markovskii, N. P. Kolesnik, Y. G. Shermolovich, *Usp. Khim.* **1987**, *56*, 1564–1583; d) R. Burgada, R. Setton in *The Chemistry of Organophosphorus Compounds* (Ed.: F. R. Hartley), Wiley-Interscience, Chichester, **1994**, pp. 185–272; e) K.-y. Akiba, *Chemistry of Hypervalent Compounds*, Wiley-VCH, New York, **1999**.

[3] a) E. L. Muetteries, W. Mahler, R. Schmutzler, *Inorg. Chem.* **1963**, *2*, 613–618; b) S. Trippett, *Phosphorus Sulfur* **1976**, *1*, 89–98; c) M. Eisenhut, H. L. Mitchell, D. D. Traficante, R. J. Kaufman, J. M. Deutsch, G. M. Whitesides, *J. Am. Chem. Soc.* **1974**, *96*, 5385–5397; d) C. G. Moreland, G. O. Doak, L. B. Littlefield, N. S. Walker, J. W. Gilje, R. W. Braun, A. H. Cowley, *J. Am. Chem. Soc.* **1976**, *98*, 2161–2165; e) G. Buono, J. R. Llinas, *J. Am. Chem. Soc.* **1981**, *103*, 4532–4540; f) L. V. Griend, R. G. Cavell, *Inorg. Chem.* **1983**, *22*, 1817–1820.

[4] a) S. Kojima, M. Nakamoto, K. Kajiyama, K.-y. Akiba, *Tetrahedron Lett.* **1995**, *36*, 2261–2264; b) S. Kojima, M. Nakamoto, K. Yamazaki, K.-y. Akiba, *Tetrahedron Lett.* **1997**, *38*, 4107–4110; c) M. Nakamoto, S. Kojima, S. Matsukawa, Y. Yamamoto, K.-y. Akiba, *J. Organomet. Chem.* **2002**, *643–644*, 441–452; d) S. Matsukawa, K. Kajiyama, S. Kojima, S.-y. Furuta, Y. Yamamoto, K.-y. Akiba, *Angew. Chem. Int. Ed.* **2002**, *41*, 4718–4722.

[5] R. S. Berry, *J. Chem. Phys.* **1960**, *32*, 933–938.

[6] For examples on P, see: a) O. Lösking, H. Willner, H. Oberhammer, J. Grobe, D. L. Van, *Inorg. Chem.* **1992**, *31*, 3423–3427; b) N. V. Timosheva, T. K. Prakasha, A. Chandrasekaran, R. O. Day, R. R. Holmes, *Inorg. Chem.* **1995**, *34*, 4525–4526; c) N. V. Timosheva, A. Chandrasekaran, T. K. Prakasha, R. O. Day, R. R. Holmes, *Inorg. Chem.* **1996**, *35*, 6552–6560; d) T. Kawashima, T. Soda, K. Kato, R. Okazaki, *Phosphorus, Sulfur Silicon Relat. Elem.* **1996**, *109–110*, 489–492; e) T. Kawashima, T. Soda, R. Okazaki, *Angew. Chem. Int. Ed. Engl.* **1996**, *35*, 1096–1098; f) P. Kommana, S. Kumaraswamy, J. J. Vittal, K. C. Kumara Swamy, *Inorg. Chem.* **2002**, *41*, 2356–2363; g) N. Satish Kumar, P. Kommana, J. J. Vittal, K. C. Kumara Swamy, *J. Org. Chem.* **2002**, *67*, 6653–6658; h) P. Kommana, N. Satish Kumar, J. J. Vittal, E. G. Jayasree, E. D. Jemmis, K. C. Kumara Swamy, *Org. Lett.* **2004**, *6*, 145–148; i) N. Satish Kumar, K. Praveen Kumar, K. V. P. Pavan Kumar, P. Kommana, J. J. Vittal, K. C. Kumara Swamy, *J. Org. Chem.* **2004**, *69*, 1880–1889; j) K. C. Kumara Swamy, K. Praveen Kumar, N. N. Bhuvan Kumar, *J. Org. Chem.* **2006**, *71*, 1002–1008; for an example of Si, see: k) E. P. A. Couzijn, M. Schakel, F. J. J. de Kanter, A. W. Ehlers, M. Lutz, A. L. Spek, K. Lammertsma, *Angew. Chem. Int. Ed.* **2004**, *43*, 3440–3442.

[7] a) I. Granoth, J. C. Martin, *J. Am. Chem. Soc.* **1979**, *101*, 4418–4622; I. Granoth, J. C. Martin, *J. Am. Chem. Soc.* **1979**, *101*, 4623–4626; b) E. F. Perozzi, R. S. Michalak, G. D. Figuly, W. H. Stevenson III, D. B. Dess, M. R. Ross, J. C. Martin, *J. Org. Chem.* **1981**, *46*, 1049–1053; c) M. R. Ross, J. C. Martin, *J. Am. Chem. Soc.* **1981**, *103*, 1234–1235.

[8] a) S. Kojima, K. Kajiyama, M. Nakamoto, K.-y. Akiba, *J. Am. Chem. Soc.* **1996**, *118*, 12866–12867; b) K. Kajiyama, M. Yoshimune, M. Nakamoto, S. Matsukawa, S. Kojima, Y. Yamamoto, K.-y. Akiba, *Org. Lett.* **2001**, *3*, 1873–1875; c) S. Kojima, M. Sugino, M. Nakamoto, S. Matsukawa, K.-y. Akiba, *J. Am. Chem. Soc.* **2002**, *124*, 7674–7675; d) S. Matsukawa, S. Kojima, K. Kajiyama, M. Nakamoto, Y. Yamamoto, K.-y. Akiba, S.-Y. Re, S. Nagase, *J. Am. Chem. Soc.* **2002**, *124*, 13154–13170; e) S. Kojima, K. Kajiyama, M. Nakamoto, S. Matsukawa, K.-y. Akiba, *Eur. J. Org. Chem.* **2006**, 218–234; f) K. Kajiyama, M. Yoshimune, S. Kojima, K.-y. Akiba, *Eur. J. Org. Chem.* **2006**, 2739–2746; g) T. Adachi, S. Matsukawa, M. Nakamoto, K. Kajiyama, S. Kojima, Y. Yamamoto, K.-y. Akiba, S. Re, S. Nagase, *Inorg. Chem.* **2006**, *45*, 7269–7277; h) X.-D. Jiang, S. Matsukawa, H. Yamamichi, K.-i. Kakuda, S. Kojima, Y. Yamamoto, *Chem. Asian J.* **2007**, *2*, 314–323.

[9] The "***exo***"/"***endo***" notation is arbitrarily based upon the position of the methyl group of the asymmetric bidentate ligand in compound **4**, and assigned to **2** and **3** so that they belong to the same series as **4** upon transformation by the thermal cyclization pathway.

[10] For examples of air- and moisture-stable diastereomeric monocyclic phosphoranes that can be purified, see: a) R. M. Moriarty, J. Hirataka, K. Liu, *J. Am. Chem. Soc.* **1990**, *112*, 8575–8577; b) R. M. Moriarty, J. Hirataka, K. Liu, A. Wendler, A. K. Awasthi, R. Gilardi, *J. Am. Chem. Soc.* **1991**, *113*, 9374–9376.

[11] "inter" and "intra" correspond to isomers involved in intermolecular hydrogen-bonding with a solvent molecule and intramolecular hydrogen-bonding with the apical oxygen atom, respectively. For X-ray structures of similar pairs of isomers, see refs.[8a,8e]

[12] a) J. Hilton, L. H. Sutcliffe, *Prog. Nucl. Magn. Reson. Spectrosc.* **1975**, *11*, 27–39; b) R. H. Contreras, M. A. Natiello, G. E. Scuseria, *Magn. Reson. Rev.* **1985**, *9*, 239–321; c) R. H. Contreras, J. C. Facelli, *Annu. Rep. NMR Spectrosc.* **1993**, *31*, 255–356.

[13] Using $\Delta G = -RT\ln K$ at $T = 300$ K and assuming a ratio of 99:1 to be the detectable minimum.

[14] The polarities of the solvents are as follows: *p*-xylene: E_T^N = 0.074, PhCN: E_T^N = 0.333; DMSO: E_T^N = 0.444. For E_T^N, see: C. Reichardt, *Solvents and Solvent Effects in Organic Chemistry*, 3rd ed., Wiley-VCH, Weinheim, **2003**.

[15] There are no grounds on which to deny the operation of alternative mechanisms such as the turnstile rotation. However, unlike the BPR mechanism, there are no general guidelines for the qualitative evaluation of specific permutational steps, which makes an analysis extremely difficult. Furthermore, a BPR description fits perfectly with our experimental results as presented in the main text. Thus, we favored to explain these results by using the BPR mechanism. For leading references involving the turnstile mechanism for pentacoordinate compounds, see: a) I. Ugi, D. Marquarding, H. Klusacek, P. Gillespie, F. Ramirez, *Acc. Chem. Res.* **1971**, *4*, 288–296; b) P. Gillespie, P. Hoffman, H. Klusacek, D. Marquarding, S. Pfohl, F. Ramirez, E. A. Tsolis, I. Ugi, *Angew. Chem. Int. Ed. Engl.* **1971**, *10*, 687–715; c) F. Ramirez, I. Ugi, *Adv. Phys. Org. Chem.* **1971**, *9*, 25–126; d) R. R. Holmes, *Acc. Chem. Res.* **1972**, *5*, 296–303; e) P. Gillespie, F. Ramirez, I. Ugi, D. Marquarding, *Angew. Chem. Int. Ed. Engl.* **1973**, *12*, 91–119; f) J. A. Altmann, K. Yates, I. G. Csizmadia, *J. Am. Chem. Soc.* **1976**, *98*, 1450–1454; g) S.-K. Shih, S. D. Peyerimhoff, R. J. Buenker, *J. Chem. Soc., Faraday Trans. 2* **1979**, *75*, 379–389; h) P. Lemmen, R. Baumgartner, I. Ugi, F. Ramirez, *Chem. Scr.* **1988**, *28*, 451–

464; i) K. Frankcombe, K. Cavell, K. Kingsley, R. Knott, B. Yates, *Chem. Commun.* **1996**, 781–782; j) M. J. Green, G. J. P. Britovsek, K. J. Cavell, B. W. Skelton, A. H. White, *Chem. Commun.* **1996**, 1563–1564; k) A. Goller, T. Clark, *Chem. Commun.* **1997**, 1033–1034; l) J. A. Casares, P. Espinet, *Inorg. Chem.* **1997**, *36*, 5428–5431; m) H. S. Rzepa, M. E. Cass, *Inorg. Chem.* **2006**, *45*, 3958–3963.
[16] K. Mislow, *Acc. Chem. Res.* **1970**, *3*, 321–331.
[17] The two-digit numerals at the vertices correspond to the configuration bearing the substituents designated by the numbers (according to the priority rule) in the two apical positions with a clockwise array of the remaining three substituents upon viewing the apical axis from the substituent of the first of the two numerals.[2a] For the present system, the order of priority for the substituents is as follows: ***1*** = $-OC(CF_3)_2C_6H_4-$, ***2*** = $-OC^*(CF_3)(CH_3)C_6H_4-$, ***3*** = $-C_6H_4C(CF_3)_2O-$, ***4*** = $-C_6H_4C^*(CF_3)(CH_3)O-$, ***5*** = *t*Bu. Thus, diastereomers **3-*exo***, **3-*endo***, **4-*exo***, and **4-*endo*** correspond to configurations ***14***, ***41***, ***12***, and ***21***, respectively.
[18] Because a five-membered ring is unable to occupy the two apical positions simultaneously, pseudorotamers ***13***, ***31***, ***24***, and ***42*** are ruled out in this diagram.
[19] Owing to the highly strained nature of the high-energy intermediates, the transition states of single-step BPRs involving these species can be assumed to be structurally and energetically very similar to these.
[20] A. Furusaki, *Acta Crystallogr., Sect. A* **1979**, *35*, 220.
[21] C. Katayama, *Acta Crystallogr., Sect. A* **1986**, *42*, 19.
[22] *TeXsan: Single Crystal Analysis Software*, version 1.9, Molecular Structure Corporation, The Woodlands, Texas 77381, TX, **1998**. The program was previously available from Mac Science Co.

Received: October 15, 2007
Published Online: February 13, 2008

